Available online at www.sciencedirect.com
ScienceDirect
Ceramics International 34 (2008) 2121–2127
CERAMICS INTERNATIONAL
www.elsevier.com/locate/ceramint

Influence of heating curve on the sintering of alumina subjected to high-energy milling

A.S.A. Chinelatto [a,*], E.M.J.A. Pallone [b], V. Trombini [c], R. Tomasi [c]

[a] *Departamento de Engenharia de Materiais – Universidade Estadual de Ponta Grossa, Av. Gal. Carlos Cavalcanti 4748, 84.030-900 Ponta Grossa – PR, Brazil*
[b] *PPG-Engenharia e Ciência dos Materiais – Universidade São Francisco, Rua Alexandre R. Barbosa 45, 13251-900 Itatiba – SP, Brazil*
[c] *Departamento de Engenharia de Materiais – Universidade Federal de São Carlos, CP 676, 13.565-905 São Carlos – SP, Brazil*

Received 16 April 2007; received in revised form 3 July 2007; accepted 16 August 2007
Available online 22 September 2007

Abstract

The optimization of the heating curve is a suitable technique for obtain dense and fine microstructures ceramics. The work reported here investigated how the introduction of isothermal heat treatments influences the heating curve of an alumina subjected to high-energy milling. The results indicate that isothermal treatments at a temperature below the beginning of linear shrinkage cause the fine particles to disappear, narrowing the final grain size distribution and increasing the final mean grain size. However, these treatments promote the densification of agglomerates originating from the milling process, and decrease the material's final density.

Keywords: A. Sintering; B. Microstructure-final; D. Al_2O_3; High-energy milling

1. Introduction

Several processing routes have being studied for polycrystalline ceramic products of high density and small grain size [1]. These routes include colloidal powder processes with particles of controlled size [2,3], hot pressing [4] and incorporation of additives as a second phase or in solid solution [5]. However, many of these techniques are not economically viable [6], depending on the application of the final product.

Control of the heating curve to manipulate the microstructure during sintering is a route that has been studied and offers the advantage of being simple and cost-effective [1,7]. One of the routes is ''rate-controlled sintering'' [7], in which the relationship between the densification and grain growth rates is determined to identify the sintering temperature at which the densification rate is maximized [7,8]. Ragulya and Skoroklod [9] studied the rate-controlled sintering of ultrafine nickel powders, obtaining sintered samples with high densities (∼99% DT) and grain sizes smaller than 100 nm. Based on their results, they stated that rate-controlled sintering is a possible route for obtaining dense materials with nanocrystalline structures.

Fast firing [10] can produce dense materials with small grain size, minimizing the time of exposure at temperatures where grain growth is fast compared with densification [8]. This is possible because coalescence mechanisms (e.g., surface diffusion and vapor transport) generally prevail over densification mechanisms (e.g., volume diffusion and grain boundary diffusion) at low temperatures. In this case, shorter times at low temperatures reduce grain growth, so that the driving force for densification is not decreased significantly [11]. In the case of alumina [12], for example, the activation energy for densification is greater than for grain growth, and high temperature sintering is the most suitable.

Rate-controlled sintering is more efficient for non-agglomerated powders, in which the microstructure develops relatively homogeneously. However, the benefits of these techniques have proved less effective for agglomerated systems. The difficulty of obtaining homogeneous green microstructures using ultrafine powders, owing to their high degree of agglomeration, leads to inhomogeneous densification, a low densification rate and a limited final density [13–15].

* Corresponding author. Tel.: +55 42 3220 3079/3080; fax: +55 42 3220 3079.
E-mail address: adriana@uepg.br (A.S.A. Chinelatto).

0272-8842/$34.00
doi:10.1016/j.ceramint.2007.08.004

Recently, the availability of many different production routes for ultrafine and nanosized ceramic powders have led research to focus increasingly on the processing of these types of powders. Transformation processes that occur at low temperatures have been observed and studied, particularly before or at the beginning of the densification stages of sintering. These processes, which have been reported for coarsening and particle repacking [16,17], affect the subsequent sintering stages. When these processes are controlled, it is possible to obtain dense and fine microstructures. One way to control these processes is to optimize the heating curve of the material by pretreating it at low temperatures.

Some works [6,8,11] have shown that pretreatments (0 at 100 h) at low temperatures (800 °C), in which little or no densification occurs, can improve the densification, microstructure and mechanical properties of high purity aluminas with and without the addition of MgO. Such pretreatments reduce the densification rate in the initial stages of sintering. However, the benefits of the evolution of a more homogeneous microstructure are evidenced in the final stage of sintering, allowing a refinement of the final microstructure. Chen [18–20] applied a heating curve in which the ceramic body was heated to a higher temperature to achieve an intermediate density, then cooled and held at a lower temperature until it was fully dense. Using this heating curve eliminated the grain growth stage characteristic of the final stage of sintering and resulted in fully dense bodies of Y_2O_3, $BaTiO_3$ and Ni–Cu–Zn ferrites with nanometric grain sizes by sintering without the application of pressure. Ye and Li [21] also used two-step sintering to obtain alumina ceramics from nanometric powders, without pressing.

Chinelatto and Tomasi [22,23] obtained alumina with ∼98% of theoretical density, with a mean grain size of ∼550 nm sintered at 1350 °C without pressure, by heat treating at temperatures below that of the beginning of the densification stage of sintering. They found that heat treatments at temperatures below the beginning of the densification stage of sintering led to a uniform particle size distribution, promoting lower overall final grain growth and greater densification.

High-energy milling results in ultrafine powders and enhances the characteristics of the original powder [24]. This paper discusses an experimental study of the influence of isothermal heat treatments on the heating curve of an alumina subjected to high-energy milling, with the objective of obtaining a dense and homogeneous microstructure with small grain sizes. The results are compared with as-received alumina.

2. Experimental procedure

A commercial alumina (AKP-53) was subjected to 6 h of high-energy milling in a SPEX 8000 Mixer Mill, using a vial and hardened steel balls (10 mm diameter), with a ball-to-powder mass ratio of 4:1. These conditions were chosen based on previous work [25], in which an optimized relationship was identified between milling efficiency, contamination and agglomeration. The iron contamination from the milling medium was eliminated by leaching with a 20% HCl water solution, followed by successive washing-decantation with water. At the end of the washing process, the water was substituted for ethyl alcohol. The milled and washed powder was deagglomerated in 10 h of ball milling with zirconia balls in isopropyl alcohol with 0.5 wt.% PABA (4-aminobenzoic acid) and 0.5 wt.% oleic acid in a polypropylene vial, after which the powder was air-dried at room temperature under agitation. The as-received and milled powders were characterized by transmission electron microscopy (TEM – Philips-CM120), by crystallite size determination estimated by peak broadening in X-ray diffraction using the Scherrer equation [26], and by measuring the specific surface area by the BET method (Micromeritics – Gemini 2370). An X-ray diffraction analysis was performed in a SIEMENS-5100 diffractometer.

The samples for sintering were uniaxially pressed under 80 MPa into cylindrical compacts (10 mm diameter and about 5 mm height) and isostatically cold-pressed under 200 MPa. The samples were heat-treated at 600 °C in air for 1 h to eliminate organic materials introduced as processing additives or present as contamination from the vials and the milling balls. The green density of the samples was about 59 ± 1% of the theoretical density (%TD).

Sintering was performed in a NETZSCH - DIL 402C dilatometer in an air atmosphere, at a constant heating rate of 15 °C/min up to 1500 °C. Based on these results, heat treatment temperatures for as-received and milled alumina were defined for the two-step sintering.

The sintered samples were characterized based on apparent density measurements taken by the Archimedes method, on grain size measurements using an image analysis program, and on a microstructural analysis using a high-resolution scanning electron microscope (Philips XL30-FEG).

3. Results and discussion

Table 1 compares the characteristics of alumina powders subjected to high-energy milling with those of as-received alumina. The equivalent spherical diameters, obtained through the values of specific area and crystallite size obtained by X-ray diffraction (see Table 1) proved to be very dissimilar, possibly due to the presence of primary polycrystalline particles in the alumina. This difference was greater in the milled powders due to the presence of dense agglomerates formed during high-energy milling, which reduced the specific exposed surface

Table 1
Crystallite size and specific surface area of as-received alumina and high-energy milled alumina

Alumina sample	X-ray diffraction crystallite size (nm)	Specific surface area (SSA) (m^2/g)	SSA spherical equivalent particle diameter (nm)
As-received	63	12.10 ± 0.3	125
High-energy milled	14.4	31.20 ± 0.3	48

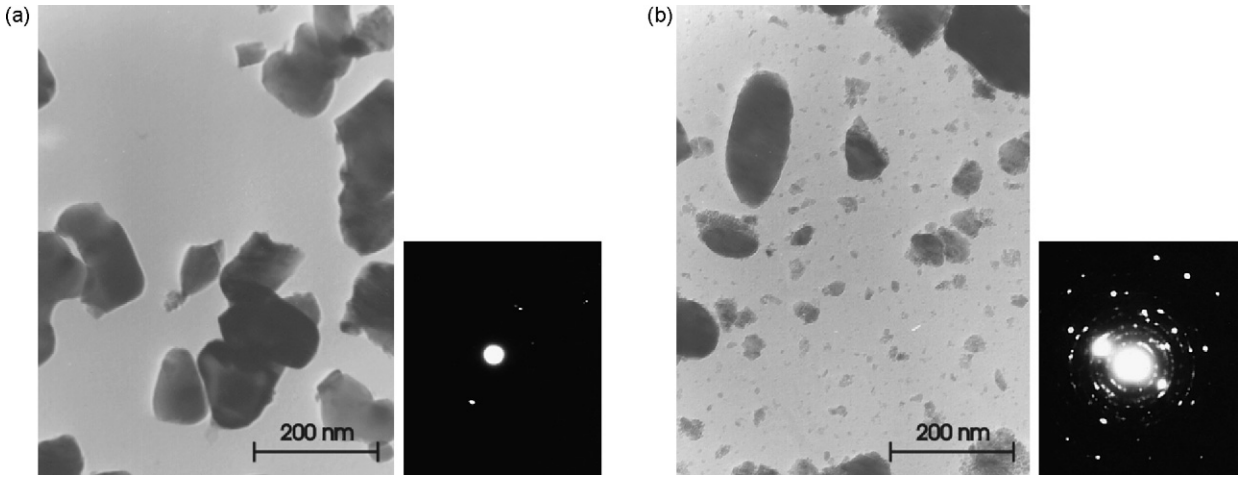

Fig. 1. TEM and electron diffraction pattern of selected area of: (a) as-received alumina, and (b) high-energy milled alumina.

area. Another possible reason for this difference was the introduction of stresses and internal deformations in the primary particles during the milling process, which caused broadening of the diffraction peaks.

The micrographs in Fig. 1(a) and (b) were obtained by transmission electron microscopy (TEM) and by the electron diffraction of selected area of the powders of as-received alumina and of alumina subjected to high-energy milling and deagglomeration. Fig. 1(b) reveals the presence of very fine powders of 10–50 nm among larger particles of up to 120 nm. The large particles are agglomerates of small particles, a finding confirmed by the electron diffraction of a selected area of the agglomerates of milled alumina powder and of the as-received alumina.

Fig. 2(a) and (b) show the variation in the linear shrinkage rate as a function of temperature for the as-received alumina and the high-energy milled alumina sintered at a constant heating rate of 15 °C/min to 1500 °C. As can be seen, the alumina subjected to high-energy milling (Fig. 2(b)) began to show a certain shrinkage rate starting at 650 °C, which was low up to approximately 1000 °C, after which the shrinkage was more marked, reaching its maximum linear rate at 1285 °C. These two stages of shrinkage were attributed to the characteristics of the milled powders, which presented agglomerates of very fine and dense crystallite with large interfacial areas, both external (measured by gas adsorption) and internal (determined by crystallite size). Because of this large surface area, surface diffusion is important at lower temperatures. However, this surface diffusion is nondensifying, tending to smooth the surface of agglomerates and to cause the finest and coarsest particles to coalescence. Thus, the slight shrinkage in this stage likely resulted from a microstructural rearrangement, which increased the densities of crystallite agglomerates. The well-known grain boundary diffusion that leads to alumina densification prevailed when the aforementioned second stage of shrinkage began. In the case of as-received alumina, shrinkage began at a higher temperature than did the milled alumina, i.e., at 1045 °C, with the maximum linear shrinkage rate occurring at 1350 °C.

One hypothesis to optimize the sintering process, which is understood as the maximization of final density with minimum grain growth, can be achieved by improving the narrowing of grain size distribution in a predensification sintering stage and producing the final densification at a maximum densification rate temperature. To confirm this hypothesis, two-step sintering experiments were carried out in the dilatometer, applying

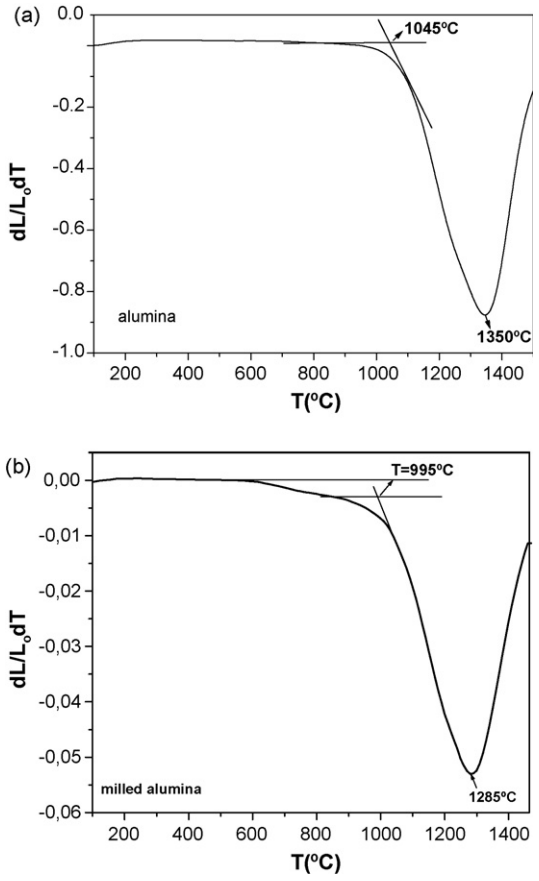

Fig. 2. Shrinkage rate versus temperature of samples sintered at a constant heating rate of 15 °C/min up to 1500 °C: (a) as-received alumina, and (b) milled alumina.

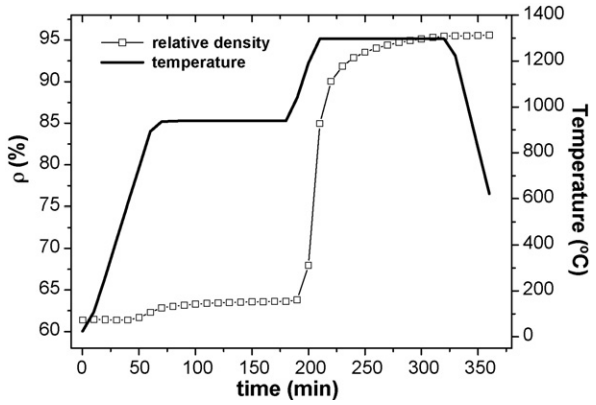

Fig. 3. Apparent density and temperature versus time under condition II.

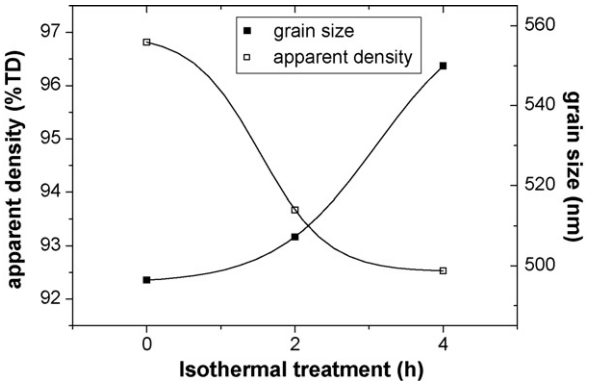

Fig. 4. Apparent densities and mean grain sizes of high-energy milled alumina sintered under conditions I, II and III.

sintering curves coherent with the temperature ranges in which the two processes, i.e., narrowing grain size distribution and final densification, were expected to occur. The following conditions were defined for the two-step sintering: for alumina subjected to high-energy milling, the first isothermal treatment at 950 °C and the second at 1300 °C (conditions I, II and III), while the first step for the as-received alumina was at 1050 °C and the second step was at the maximum sintering temperature of 1350 °C (conditions IV, V and VI). These conditions are listed in Table 2.

Fig. 3 presents the behavior of relative density (ρ) and temperature versus sintering time for condition II. The relative density during sintering was determined from green density (ρ_v) and measured shrinkage ($\Delta L/L_o$), using the approximate Eq. (1) [6], assuming that the deformation is isotropic and all axial strain is devoted to densification of the specimen [27].

$$\rho = \rho_g \times \left(1 - \frac{\Delta L}{L_o}\right)^{-3} \quad (1)$$

As can be seen in Fig. 3, no pronounced densification occurred in the first step of the isothermal treatment, despite the 2-h step at 950 °C. However, there was visible densification during heating between the first and second steps, and during the second step.

Fig. 4 depicts the apparent densities and mean grain sizes of milled alumina sintered at 950 °C for varying periods of time under conditions I, II and III, while those of the as-received alumina sintered at 1050 °C for varying periods of time under conditions IV, V and VI are shown in Fig. 5. As Fig. 5 indicates, the heat treatments of as-received alumina at temperatures slightly below the onset of shrinkage cause lower growth of the final grain and greater densification. In the high-energy milled alumina, the longer the step the lower the density attained and the larger the mean final grain size.

The largest mean grain size attained by increasing the isothermal treatment time of milled alumina at 950 °C was probably due to the surface diffusion and coalescence processes mentioned earlier. During the isothermal treatment at 950 °C, these processes were intensified, as indicated in Fig. 6(a) and (b), which shows the fracture surface of an alumina sample before and after the 2-h isothermal treatment at 950 °C. Note that the heat treatment caused the finest particles to disappear and slightly coarsened the coarsest particles, greatly decreasing the specific surface area and slightly increasing the apparent

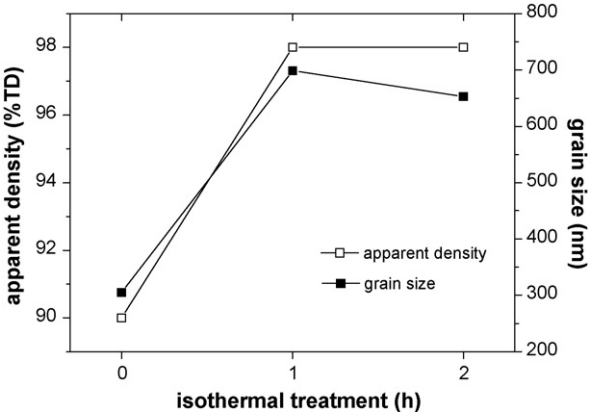

Fig. 5. Apparent densities and mean grain sizes of unmilled alumina sintered under conditions IV, V and VI.

Table 2
Parameters defining the heating curves used in the sintering experiments of the samples prepared with as-received and high-energy milled alumina

	Condition	Isothermal treatment 1 (°C)	Time (h) Step 1	Isothermal treatment 2 (°C)	Time (h) Step 2
Milled alumina	I	–	–	1300	2
	II	950	2	1300	2
	III	950	4	1300	2
As-received alumina	IV	–	–	1350	2
	V	1050	1	1350	2
	VI	1050	2	1350	2

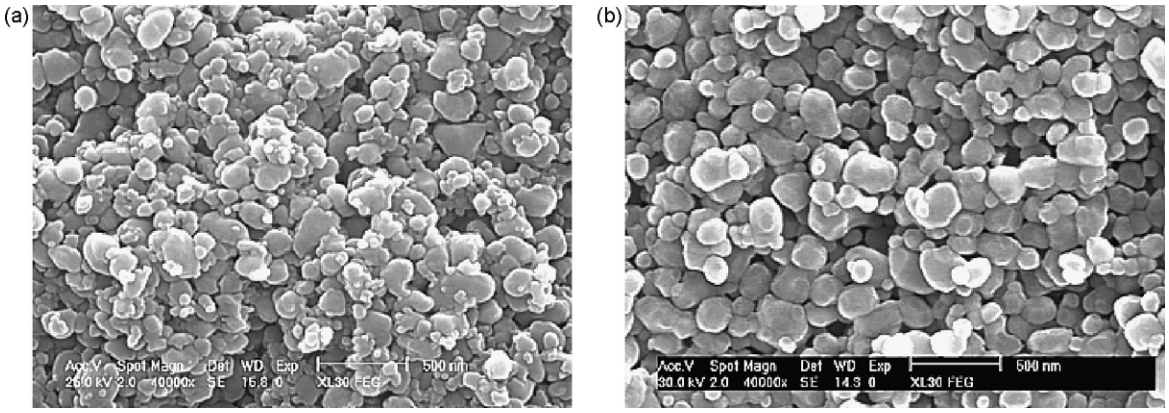

Fig. 6. SEM images of fracture surfaces of high-energy milled alumina samples: (a) without isothermal treatment at 950 °C, and (b) with isothermal treatment at 950 °C for 2 h.

density, as indicated in Table 3. This increase in apparent density probably resulted from a microstructural rearrangement that increased the agglomerate density.

The effect of nondensifying surface diffusion and particle coalescence processes during the isothermal treatment not only promoted a small increase in the mean grain size but also affected the final grain size distribution of the milled alumina, as indicated in Fig. 7(a), which shows the grain size distribution curve of milled alumina sintered under conditions I and II. The grain size distribution in the condition I, without heat treatment, is broader with a standard deviation of 140 μm. In contrast, in the condition II, with longer heat treatments at 950 °C, the grain size distribution became narrower, with a standard deviation of 90 μm. In as-received alumina, the grain size distribution was also narrowed but the mean grain size was reduced (Fig. 7(b)).

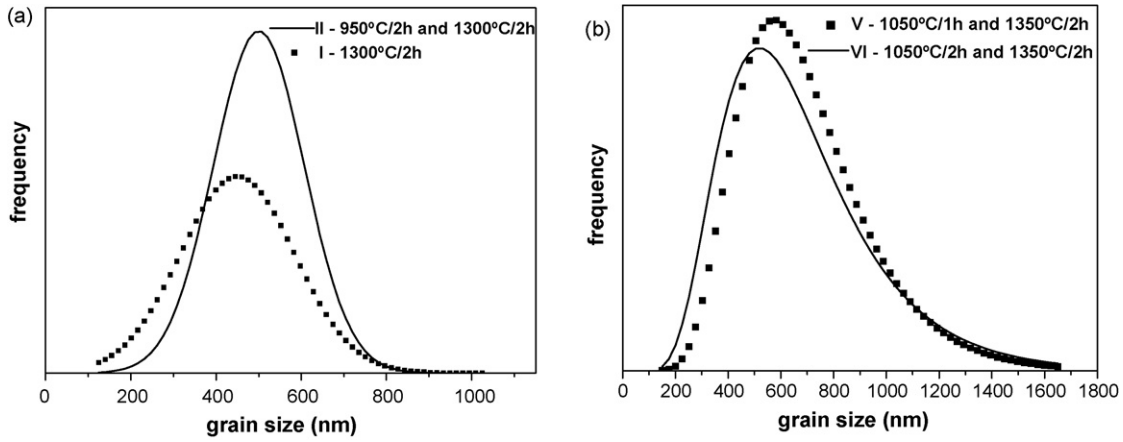

Fig. 7. Grain size distribution of: (a) high-energy milled alumina sintered under conditions I and II, and (b) as-received alumina sintered under conditions V and VI.

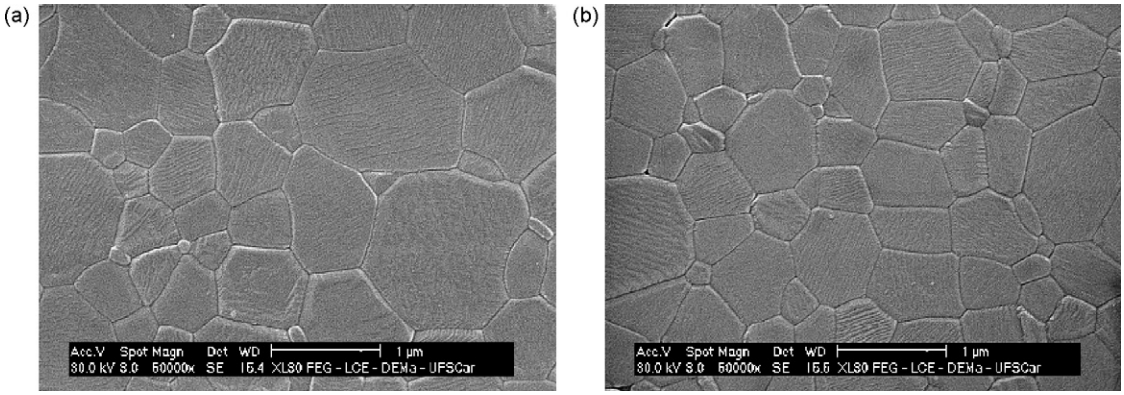

Fig. 8. SEM images of high-energy alumina samples sintered for 2 h at 1300 °C: (a) without isothermal treatment at 950 °C, and (b) with 2 h of isothermal treatment at 950 °C.

Table 3
Specific surface area and apparent density of high-energy milled alumina without isothermal treatment at 950 °C and of high-energy milled alumina isothermally treated at 950 °C for 2 h

	Without treatment	950 °C/2 h
Specific surface area (m^2/g)	31.2 ± 0.3	9.7 ± 0.3
Apparent density (%DT)	59.0 ± 0.2	61.0 ± 0.2

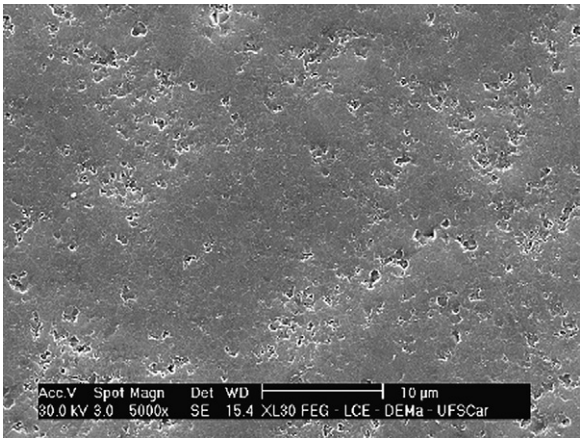

Fig. 9. SEM image of the sample sintered under condition II.

Fig. 8 presents microstructures of alumina samples subjected to high-energy milling and sintered with and without isothermal treatment at 950 °C, i.e., under conditions I and II, respectively. The considerable homogeneity of the final microstructure achieved by introducing an isothermal treatment at 950 °C can be observed in these figures.

In the milled alumina, the densification of agglomerates generates areas of different densities in the sample, which is intensified as the time of low temperature isothermal treatment increases, causing the density to decrease as the isothermal treatment time increases. A micrograph of the sintered sample under condition II, presented in Fig. 9, shows the presence of large pores. These large pores probably originated from agglomerates densified during the low temperature isothermal treatment and also from packing defects occurring during the preparation of the samples, due to agglomeration of the milled products. These pores were not eliminated even after long sintering times.

4. Conclusion

The introduction of isothermal treatments in the heating curve of an alumina at temperatures below the beginning of an accentuated shrinkage process influenced the development of the final microstructure, promoting a microstructural refinement of alumina compacts. The isothermal treatment promoted particle coalescence, narrowing the final grain size distribution. During the isothermal treatment of high-energy milled alumina, the apparent density increased probably due to particle repacking, which resulted in increased agglomerate density. Because of agglomerate densification during the isothermal treatment, and the inherent agglomeration of high-energy milled powders, it was not possible to reach high final densities.

Acknowledgements

We would like to thank the Brazilian institutions CNPq, CAPES and FAPESP for their financial support of this work.

References

[1] R.J. Brook, Fabrication principles for the production of ceramics with superior mechanical properties, Proc. Br. Ceram. Soc. 32 (1982) 7–24.
[2] W.M. Sigmund, N.S. Bell, L. Bergström, Novel powder-processing methods for advanced ceramics, J. Am. Ceram. Soc. 83 (2000) 1557–1574.
[3] L.C. Lim, P.M. Wong, J. Ma, Colloidal processing of sub-micron alumina powder compacts, J. Mat. Proc. Tec. 67 (1997) 137–142.
[4] Z. He, J. Ma, Grain growth rate constant of hot-pressed alumina ceramics, Mater. Lett. 44 (2000) 14–18.
[5] H. Erkalfa, Z. Misirk, T. Baykara, Effect of additives on the densification and microstructural development of low-grade alumina powders, J. Mat. Proc. Tec. 62 (1996) 108–115.
[6] F.J.T. Lin, L.C. DeJonghe, Microstructure refinement of sintered alumina by two-step sintering technique, J. Am. Ceram. Soc. 80 (1997) 2269–2277.
[7] R.M. German, Sintering Theory and Practice, John Wiley & Sons, New York, 1996.
[8] M.-Y. Chu, L.C. DeJonghe, M.K.F. Lin, F.J.T. Lin, Precoarsing to improve microstructure and sintering of powder compacts, J. Am. Ceram. Soc. 74 (1991) 2902–2911.
[9] A.V. Ragulya, V.V. Skorokhod, Rate-controlled sintering of ultrafine nickel powder, Nanostruct. Mat. 5 (1995) 835–843.
[10] M.P. Harmer, R.J. Brook, Fast firing microstructural benefits, J. Br. Ceram. Soc. 80 (1981) 147–148.
[11] F. Lin, L.C. DeJonghe, Initial coarsening and microstructural evolution of fast-fired and MgO-doped alumina, J. Am. Ceram. Soc. 80 (1997) 2891–2896.
[12] M.P. Harmer, E.W. Roberts, R.J. Brook, Rapid sintering of pure and doped α-Al_2O_3, J. Br. Ceram. Soc. 78 (1979) 22–25.
[13] A. Rosen, H.K. Bowen, Influence of various consolidation techniques on the green microstructure and sintering behavior of alumina powders, J. Am. Ceram. Soc. 71 (1988) 970–977.
[14] S. Inada, T. Kimura, T. Yamaguchi, Effect of green compact structure on the sintering of alumina, Ceram. Int. 16 (1990) 369–373.
[15] F.W. Dynys, T.W. Hallonen, Influence of aggregates on sintering, J. Am. Ceram. Soc. 67 (1984) 596–601.
[16] P.-L. Chen, I.-W. Chen, Sintering of fine oxide powders. I. Microstructural evolution, J. Am. Ceram. Soc. 79 (1996) 3129–3141.
[17] P.-L. Chen, I.-W. Chen, Sintering of fine oxide powders. II. Sintering mechanism, J. Am. Ceram. Soc. 80 (1997) 637–645.
[18] I.-W. Chen, X.H. Wang, Sintering dense nanocrystalline ceramics without final-stage grain growth, Nature 404 (2000) 168–171.
[19] X.-H. Wang, P.-L. Chen, I.-W. Chen, Two-step sintering of ceramics with constant grain-size. I. Y_2O_3, J. Am. Ceram. Soc. 89 (2006) 431–437.
[20] X.-H. Wang, X.-Y. Deng, H.-I. Bai, H. Zhou, W.-G. Qu, L.T. Li, I.-W. Chen, Two-step sintering of ceramics with constant grain-size II. $BaTiO_3$ and Ni–Cu–Zn ferrite, J. Am. Ceram. Soc. 89 (2006) 438–443.
[21] J. Li, Y. Ye, Densification and grain growth of Al_2O_3 nanoceramics during pressureless sintering, J. Am. Ceram. Soc. 89 (2006) 139–143.
[22] R. Tomasi, L. Del Prette, L.A.S.A. Chinelatto, Influence of atmosphere and heating curve on microstructure evolution during sintering of submicron alumina powder, in: Presented at the 103rd Annual Meeting of the American Ceramic Society, Indianapolis, Indiana, April 23, 2001 (Paper No BSD8A-13-2001).
[23] A.S.A. Chinelatto, Sinterização de pós ultra finos de alumina para a obtenção de cerâmicas densas e com pequenos tamanhos de grãos, in: Tese

de doutorado em Ciência e Engenharia de Materiais, Universidade Federal de São Carlos, São Carlos, 2002.
[24] R. Tomasi, A. Rabello, A.S.A. Chinelatto, L. Reis, W.J. Botta F°, Characterization of high energy milled alumina powder, Cerâmica 44 (1998) 66–70.
[25] A.P. Nakajato, E.M.J.A. Pallone, A.S.A. Chinelatto, W.J. Botta Fo, R. Tomasi, Pós nanométricos obtidos por moagem reativa, in: Anais do 13° Congresso Brasileiro de Ciência e Engenharia de Materiais, 1998, 5260–5269.
[26] T.R. Malow, C.C. Koch, Grain growth in nanocrystalline iron prepared by mechanical attrition, Acta Mater. 45 (1997) 2177–2186.
[27] R. Ray, Separation of cavitation-strain and creep-strain during deformation, J. Am. Ceram. Soc. 65 (1982) C46.